

Simulating evoked gamma oscillation of human EEG in a network of spiking neurons reveals an early mechanism of memory matching

Ingo Fründ and Christoph S. Herrmann

Department for Biological Psychology, Institute of Psychology, Otto-von-Guericke University, Magdeburg, Germany

Abstract. Stimulus-locked gamma oscillations in early visual cortex have experimentally been linked to fast matching with perceptual memory. It has been argued that these oscillations could be explained by recurrent feedback between different levels of visual processing. We simulated two layers of simple spiking neurons in a minimal network. Synaptic strengths of feedforward as well as feedback connections were systematically varied. The network was stimulated with patterns that were either completely or partially represented by convergent connections between the layers, or that were not represented in the connectivity pattern of the network. Transient, stimulus-locked spike trains with a frequency of ≈ 40 Hz were observed for stimuli that were represented in the connectivity pattern of the network, but not for stimuli that were not represented in the connectivity pattern.

Keywords: Evoked gamma oscillation, memory matching, spiking neuron

PACS: 87.19.LA Neuroscience

INTRODUCTION

The world around us is constantly changing. To keep track of these changes we are required to rapidly differentiate familiar from unfamiliar stimuli. The former can be used to analyze the behavioral demands of the current situation whereas the latter will need to be learned if they turn out to be behaviorally important. At best, a mechanism that differentiates familiar from unfamiliar stimuli should already provide the brain with a coarse idea of the identity of the familiar stimuli. Here we propose a mechanism that could differentiate familiar from unfamiliar stimuli based on a rate code across a whole group of neurons. At the same time coding the identity of the familiar stimuli is performed in the spike patterns of single neurons.

Recently, stimulus locked, evoked gamma band oscillations (≈ 40 Hz) have been shown to be modulated by the familiarity of visual stimuli [1]. If the participants of this study watched line drawings of real world objects, a strong evoked gamma band response (eGBR) was measured from electroencephalographic electrodes over posterior cortex regions. The eGBR was significantly diminished for randomized versions of the same line drawings. Evoked GBRs vary with physical parameters of a stimulus, such as size and eccentricity [2]. It has been argued that these properties suggest the origin of eGBRs to be at an early stage of visual processing. Thus, it seems reasonable that the memory effects reported by Herrmann et al. [1] occur early in the visual processing hierarchy. However, cells in early visual areas usually code for elementary stimulus features such as orientation or spatial frequency rather than familiar or unfamiliar objects. Different authors argued that recurrent activation from higher visual areas might disambiguate upstream information in lower visual areas [3, 4]. Such feedback mechanisms have been proposed as a basis for the enhanced eGBR to familiar stimuli [5].

In the current report, we explore how recurrent feedback might alter early visual processing. We use a minimal two layer network of simple spiking neurons [6] and systematically vary the strength of feedback and feedforward connections. This model is stimulated with spike trains that resemble those measured in the lateral geniculate nucleus of the thalamus [7]. We compared spike responses to stimulus configurations that match with the pattern of convergent connections in the network (like stimuli a and b in Figure 1) with configurations that do not match with this pattern (e.g. stimulus c in Figure 1).

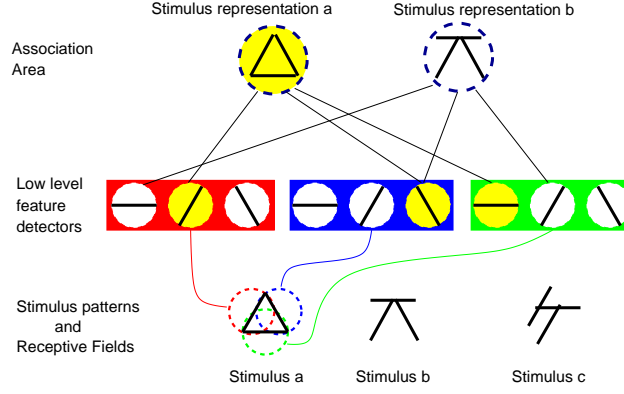


FIGURE 1. Minimalistic network of feature detectors that might be responsible for memory matching. In the middle of the figure low level feature detectors are indicated. The red, blue and green boxes indicate the location of the receptive field (RF) of these feature detectors that are depicted in the lower part of the figure. The top of the figure displays detectors for three different complex patterns. The black lines that connect the complex patterns at the top of the figure with the feature detectors at the center represent hypothetical synapses. Note how these synapses render stimuli a and b known to the network. No synapses converge to stimulus c. Thus stimulus c is not represented in the memory of the network. Cells that are activated by the square at the bottom of the figure are colored yellow.

METHODS

Neuron model. It has been argued that coding schemes that are entirely based on a rate code are not fast enough to account for the rapid recognition times observed in the visual system [8]. In order to retain the characteristics of single neurons, we modeled spiking neurons using a qualitative, yet biologically plausible neuron model [6]. This model is characterized by two coupled differential equations

$$\frac{dv}{dt} = 0.04v^2 + 5v + 140 - u + I, \quad \frac{du}{dt} = a(bv - u) \quad (1)$$

with the auxiliary after-spike resetting, if $v \geq 30$ mV, then $v \leftarrow c$ and $u \leftarrow u + d$. The variable v represents the membrane potential of the neuron and u represents a membrane recovery variable, which accounts for the activation of K^+ ionic currents and inactivation of Na^+ ionic currents. Using the four parameters a, b, c and d excitatory neurons have been tuned to mimic the dynamics of regular spiking cortical neurons and inhibitory neurons have been tuned to mimic the dynamics of fast spiking neurons¹[6].

Synaptic connections. Twenty spiking neurons were connected to form two levels of processing. Connections between the two levels formed the convergent-divergent connection scheme depicted in Fig. 2. Each three cells in level I formed convergent excitatory connections to one cell in level II. At the same time cells in level II projected backward to those cells in level I that excited them. Excitatory cells were grouped into small ensembles of 4 cells which inhibited each other.

Synaptic currents were modeled using

$$I_{\text{syn}} = g_{\text{AMPA}}(v - 0) + g_{\text{NMDA}} \frac{((v + 80)/60)^2}{1 + ((v + 80)/60)^2} (v - 0) + g_{\text{GABA}_A} (v + 70) + g_{\text{GABA}_B} (v + 90), \quad (2)$$

where $dg./dt = -g./\tau$, with $\tau = 5, 150, 6$ or 150 ms for the simulated AMPA, NMDA, $GABA_A$ and $GABA_B$ receptors respectively [9]. Synaptic currents were computed for every synapse individually and the sum of all incoming currents was inserted in equation (1).

If a spike was emitted at the presynaptic neuron, the corresponding conductance g was incremented by a value w after a conduction delay Δ . If the presynaptic neuron was inhibitory, g_{GABA_A} and g_{GABA_B} were incremented, if it was

¹ We ran the model with different neuron parameters, but did not observe qualitative differences in the results.

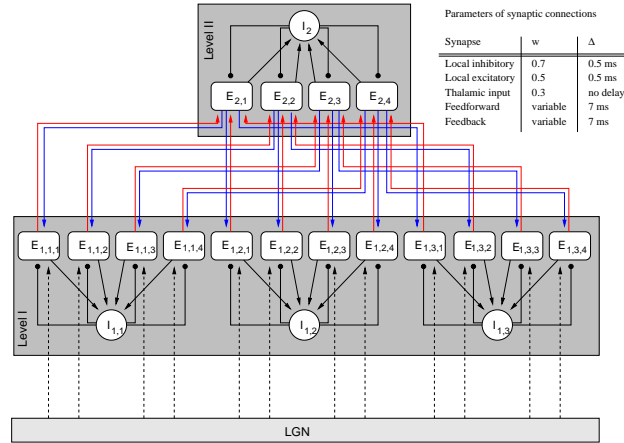


FIGURE 2. Topology of the network under study. Arrow heads indicate excitatory, black dots inhibitory connections. Cells marked with E represent excitatory, regular spiking neurons, cells marked with I represent inhibitory, fast spiking neurons. Red connections mark feedforward, blue connections feedback propagation. The inlay shows parameters of the employed synaptic connections.

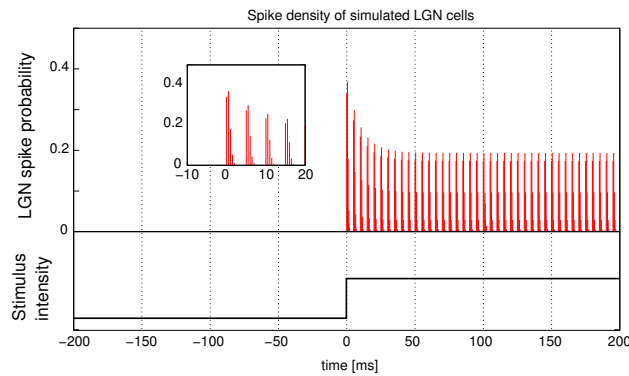


FIGURE 3. Spike density of thalamic spike trains. The small graphic represents the time around stimulus onset. Stimulus onset is at 0 ms.

excitatory, g_{AMPA} and g_{NMDA} were incremented. The values w and Δ were assigned individually for each synapse. w represents the strength of that synapse. The assignments for w and Δ are summarized in the table at the top right of Figure 2. Synapses from level I to level II will be called feedforward connections, synapses from level II to level I will be called feedback connections. The strength w of feedforward and feedback connections was systematically varied in the simulation. The delay Δ was set in accordance with data summarized by Bullier [3].

Thalamic input. Thalamic input was modeled in accordance with reports on response characteristics of the lateral geniculate nucleus of the thalamus [7]. The time after stimulus onset was split into subsequent intervals of length 5ms. For each interval we ascertained (i) the probability that a spike would be emitted in this interval and (ii) the timing of that spike. To determine whether a spike was emitted, the transient response of the thalamus was modeled as $1 - \gamma$, where $d\gamma/dt = 0.1(-\gamma + 0.5)$. This transient response was used as the probability for a given LGN cell, to emit a spike within a 5ms interval starting at the specified time. If a spike was emitted, the exact timing of the spike within the 5ms interval was set to $t_{\text{spike}} = t_{\text{start}} + 0.5N$, where N was taken from a binomial distribution with parameters (10, 0.1), and t_{start} represents the beginning of the 5 ms interval. The resulting spike density function of this procedure is plotted in Figure 3. The spike rate decays from initially approximately 200 Hz to a constant rate of 100 Hz. All simulations were run with 10 different seeds for the random number generator to compensate for specific effects of the LGN spike trains. LGN cells were not modeled in detail. Feedback from cortical cells to LGN cells was neglected.

Three different types of stimuli were applied. Familiar stimuli, that matched with the convergent-divergent topology

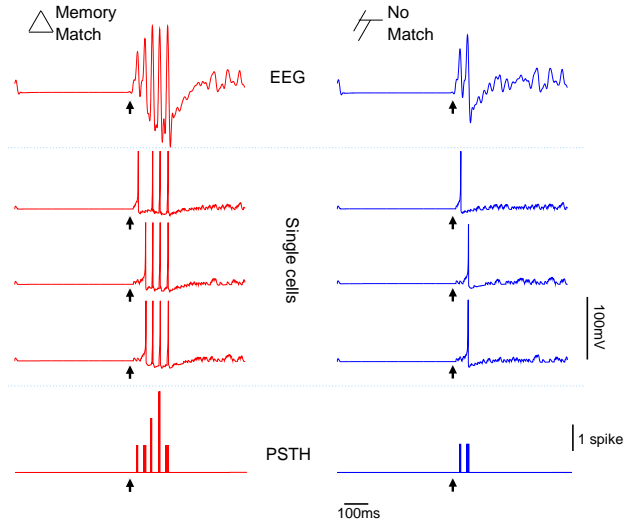


FIGURE 4. Data postprocessing. In the center of the figure the time courses of the membrane potential of three different neurons are displayed. At the top of the figure the sum of the lowpassfiltered single neuron responses is displayed. This corresponds roughly to local EEG signals. The bottom of the figure shows PSTHs across all the displayed neurons. Responses to a matching stimulus are displayed on the right side (red), responses to a non matching stimulus are displayed on the left side (blue).

of the network were modeled as spike trains applied to cells $E_{1,k,l}$, where $k = 1, 2, 3$ and l constant (see Figure 2), e.g. $\{E_{1,1,1}, E_{1,2,1}, E_{1,3,1}\}$. Note how these cells converge to one cell $E_{2,l}$ in the second level. To simulate unfamiliar stimuli, not matching with the network topology, again three cells $E_{1,k,l}$, $k = 1, 2, 3$ were stimulated. However, this time the index l differed for all three stimulated cells, e.g. $\{E_{1,1,1}, E_{1,2,2}, E_{1,3,3}\}$. Note that these three cells all project to different cells in the second level in Figure 2. To mimic degraded versions of familiar patterns, that partially matched with the network topology, we applied a third stimulation paradigm. Again three excitatory cells in the first level received LGN spike trains. However, this time the spike trains were applied to cells $E_{1,k,l}$, $k = 1, 2, 3$, where $l \in \{l_1, l_2\}$, e.g. $\{E_{1,1,1}, E_{1,2,1}, E_{1,3,2}\}$. For shorter notation stimuli will only be denoted by the tuple of values, the parameter l takes. Thus $(1, 1, 1)$ would be a matching, $(1, 2, 3)$ a non-matching and $(1, 2, 2)$ a partially matching stimulus.

Data postprocessing. To compare the network responses to different stimuli, we computed peri-stimulus time histograms (PSTH) across all neurons in level I. To compute these histograms the number of spikes was counted in bins of 5 ms length. Figure 4 illustrates this process. In order to track the changes of the PSTHs with varying feedback or feedforward strength, the PSTHs were color coded and compiled into a plane spanned by the time of the bin and the feedback/feedforward strength.

RESULTS

The responses of the excitatory cell $E_{1,1,1}$ to stimuli $(1, 1, 1)$ and $(1, 2, 3)$ are displayed in Figure 5. Note that the responses are virtually the same until feedback activity comes into play after approximately 90 ms. Figure 4 shows responses from three different cells to a matching (red) and a non matching stimulus (blue). Note that the responses of the cells are highly time-locked to the onset of the stimulus, although this is not necessarily the case for the first spike.

Variation of feedback connections. To explore the effect of feedback, we fixed the feedforward connection strength to a value $w = 0.55$ and varied the strength of feedback connections between 0 and 3. The left row of Figure 6 displays the effects of feedback variation on the response patterns to the different stimulus classes. If feedback strength exceeded a value of about 1, transient regular spike trains with a spike frequency of ≈ 40 Hz emerged approximately 50 ms after stimulus onset. These spike trains showed nearly no jitter for different LGN spike trains and were highly phase locked to the onset of the stimulus. For stronger feedback longer spike trains emerged, with the same frequency. Stimuli that did not match with the network topology could not trigger any oscillatory activity. Partially matching stimuli triggered shorter spike trains with the same spike frequency.

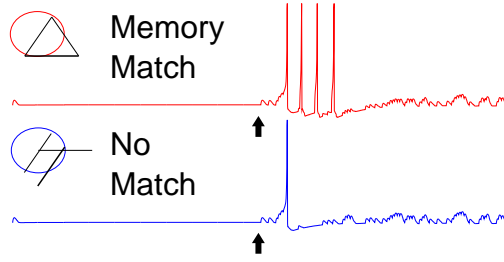


FIGURE 5. Time course of the membrane potential of excitatory cell $E_{1,1,1}$ in response to the matching stimulus (1,1,1) (red line) and the non-matching stimulus (1,2,3) (blue line). The small black arrow indicates the onset of the stimulus. Note that LGN input is the same in both cases.

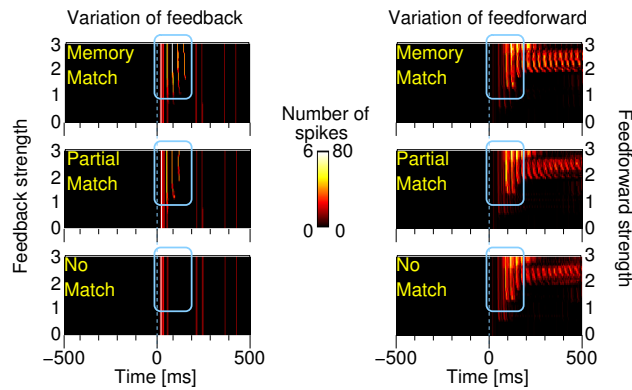


FIGURE 6. PSTHs for variation of feedback (left column) and feedforward strength (right column). On the abscissa the time is indicated, on the ordinate the varying synapse strength w . The number of spikes that were emitted in the whole first level within a time window of 5 ms is coded by the color. The first row displays results for stimulation with matching stimuli, the second row displays results for stimulation with non-matching stimuli and the third row displays results for partially matching stimuli. Runs with 10 different initializations of the random number generator have been used to estimate the PSTHs. Note that for increasing feedback strength matching, partially matching and not matching stimuli differ early after the stimulus (light blue boxes). For variation of feedforward excitation, excessive spiking that did not differentiate between stimuli, was found for all conditions.

Variation of feedforward connections. To explore the effects of feedforward activity, the strength of feedback connections was fixed to a value of $w = 1.5$, while the strength of feedforward connections was varied between $w = 0$ and $w = 3$. As shown in the right display of Figure 6, stronger feedforward connections were associated with excessive spike activity. However, the spike patterns did not differentiate between the three stimulus categories.

DISCUSSION

In the current study, we present a minimal model for the emergence of stimulus locked gamma oscillations (≈ 40 Hz). Stimulus locked gamma oscillations were observed in response to stimuli that matched with the network topology, but not for stimuli that were not represented by the network topology.

Simulating EEG data. Recently effects of familiarity on early, stimulus locked gamma oscillations have been reported for electroencephalogram (EEG) recordings [1]. It has been argued that recurrent feedback might be relevant to account for the observation, that eGBRs are stronger in response to known stimuli [5]. Here we employ a spiking neuron model to suggest, that this might indeed be the case. We use a physiologically realistic neuron model, that displays spiking and bursting behaviour [6] and biologically plausible conduction delays as have been reported for interareal connections within the visual pathway [3]. However, there is some difference between the data reported here and the data recorded using EEG. The EEG represents the common activity of huge numbers of neurons [10], whereas the model presented here incorporates no more than 20 cells. In order to model EEG phenomena usually neural field

equations are employed, that do not explicitly contain single neurons anymore [11, 12, 13, 14]. We decided to model single spiking neurons in order to analyze both, spike timing and spike rate. A question for future research will be how these effects can be translated to neural field equations.

Two levels of coding. Having access to both, spike timing and spike rate of our network, we could demonstrate that both, single spikes as well as spike rate carry information that might be relevant for the organism. It has been argued that only codes that rely on single spikes of each neuron can account for the incredibly fast recognition times that can be observed experimentally [8]. Others have argued that adaptive behaviour requires the dynamics of neural mass as recorded using EEG and modeled by field equations [15, 11]. The minimal network presented here actually combines these approaches. Information about the actual stimulus is contained in the spike patterns of single neurons, whereas the summed activity of all cells in level I contains information about the success of the recognition and thus about the necessity for learning.

Outlook. How can the convergent-divergent connectivity pattern employed in this study be learned? A learning rule based on spike-timing dependent plasticity [16] would most probably not work properly. The learning effects due to the processing in one direction (e.g. feedforward) and the unlearning effects due to processing in the other direction (e.g. feedback) would counteract each other leading to no learning at all. One possible solution might be to use separate subsystems for feedforward and feedback processing. In this case synapses within the feedforward subsystem would only learn feedforward processing, whereas synapses in the feedback subsystem would only learn feedback processing. At every level of visual processing such a system would integrate information from the two subsystems. Processing streams for separate feedforward and feedback processing have been associated with the layer structure of the cortex [4]. However, another solution to this problem might be to restrict the time intervals during which learning can occur or to restrict the number of synapses that can learn. As a possible candidate to switch the whole network between different types of memory processing, low frequency oscillations in the theta range (5-7 Hz) have been discussed [see 17, for review]. A plausible mechanism for selection of only a subset of the neurons for learning, backpropagating calcium spikes have been proposed [18]. In this model only those cells can modulate their synapses, that are not inhibited in a short time window after generating an action potential. By including inhibition, this learning rule incorporates information about the state of the whole network. Although initially proposed for feedforward processing this idea has recently been extended to hierarchical network topologies that include feedback and symbolic representations[19].

Conclusion. Together our results indicate that memory effects on early, stimulus-locked gamma responses can be explained by feedback effects within the visual pathway.

REFERENCES

1. C. S. Herrmann, D. Lenz, S. Junge, N. A. Busch, and B. Maess, *BMC Neuroscience* **5** (2004).
2. N. A. Busch, S. Debener, C. Kranczioch, A. K. Engel, and C. S. Herrmann, *Clin Neurophysiol* **115**, 1810–1820 (2004).
3. J. Bullier, *Brain Res Rev* **36**, 96–107 (2001).
4. E. Körner, M.-O. Gewaltig, U. Körner, A. Richter, and T. Rodemann, *Neural Networks* **12**, 989–1005 (1999).
5. C. S. Herrmann, M. H. Munk, and A. K. Engel, *Trends in Cognitive Science* **8**, 347–355 (2004).
6. E. M. Izhikevich, *IEEE Transactions on neural networks* **14**, 1569–1572 (2003).
7. K. Funke, and F. Wörgötter, *Prog Neurobiol* **53**, 67–119 (1997).
8. S. Thorpe, A. Delorme, and R. Van Rullen, *Neural Networks* **6-7**, 715–725 (2001).
9. E. M. Izhikevich, J. A. Gally, and G. M. Edelman, *Cereb Cortex* **14**, 933–944 (2004).
10. P. L. Nunez, and R. Srinivasan, *Electric Fields Of The Brain.*, Oxford University Press, 2006, 2nd edn.
11. W. J. Freeman, *Mass Action in the Nervous System. Examination of the Neurophysiological Basis of Adaptive Behavior through the EEG*, ACADEMIC PRESS, New York, 1975.
12. V. K. Jirsa, and H. Haken, *Physica D* **99**, 503–526 (1997).
13. P. A. Robinson, C. J. Renni, D. L. Rowe, S. C. O'Connor, J. J. Wright, E. Gordon, and R. W. Whitehouse, *Neuropsychopharmacol* **28**, 74–79 (2003).
14. D. L. Rowe, and J. J. Wright, *Behav Brain Sci* **24** (2002).
15. W. J. Freeman, and L. J. Rogers, *J Neurophysiol* **87**, 937–945 (2002).
16. G.-q. Bi, and M.-m. Poo, *J Neurosci* **18**, 10464–10472 (1998).
17. M. Lengyel, Z. Huhn, and P. Érdi, *Biol Cybern* **92**, 393–408 (2005).
18. K. P. Körding, and P. König, *Neural Networks* **13**, 1–9 (2000).
19. P. König, and N. Krüger, *Biological Cybernetics* **94**, 325–334 (2006).